Episodic experience drives ripple reorganization and synaptic changes in the hippocampus

Junko Ishikawa[1], Takuto Tomokage[1], and Dai Mitsushima[1,2,*]

[1] Department of Physiology, Yamaguchi University Graduate School of Medicine, Yamaguchi, 755-8505, Japan.
[2] The Research Institute for Time Studies, Yamaguchi University, Yamaguchi, 753-8511, Japan.

Corresponding authors:
Prof. Dai Mitsushima, e-mail: mitsu@yamaguchi-u.ac.jp

CONFLICT OF INTEREST
The authors declare no competing interests.

Ethical statement:
Our manuscript confirming the study is reported in accordance with ARRIVE guidelines (https://arriveguidelines.org).

Data availability statement:
Any additional information required to reanalyze the data reported in this paper is available from the lead contact upon request. Although the data are not publicly available due to the inclusion of data for ongoing research, all data will be uploaded to the web server of the Yamaguchi University Graduate School of Medicine upon acceptance of the research paper. In addition, all data will be deposited in an open repository.

ABSTRACT

The hippocampus plays a key role in encoding episodic memory by transforming recent experience into persistent neuronal and synaptic modifications. However, the physiological processes that link real-world experience to network-level and cellular-level changes remain incompletely understood. Here, we investigated how distinct types of episodic experience reorganize ensemble firing dynamics and synaptic input in the hippocampal CA1 region of freely moving rats.

We identified spontaneous "super bursts"—brief episodes of high-frequency firing across neuronal populations—that emerged specifically during emotionally salient experiences. These bursts were followed by increased ripple firings, characterized as short, synchronous events associated with memory consolidation. Using information entropy analysis, we found that ripple firing patterns became more diverse after experience, indicating enhanced variability in neural representation. Ex vivo whole-cell patch-clamp recordings revealed that miniature excitatory and inhibitory synaptic currents in CA1 pyramidal neurons also underwent experience-specific reorganization.

Together, these findings propose a cascading mechanism in which episodic experience triggers coordinated ensemble activity, leading to ripple reorganization and synaptic remodeling, thereby contributing to the initial encoding of memory. Our study integrates systems-level neuronal dynamics with cellular-level synaptic plasticity, offering new physiological insights into how brain circuits adapt to experience.

Key points:

- The hippocampal CA1 region encodes episodic memory through experience-dependent changes in neuronal activity and synaptic input.
- Distinct episodic experiences evoke high-frequency "super bursts" in CA1, followed by diversification of ripple firing patterns.
- Information entropy of ripple firings increased after experience, suggesting enhanced representational diversity.
- Ex vivo recordings revealed experience-specific reorganization of excitatory and inhibitory synaptic currents in CA1 pyramidal neurons.
- These findings propose a cascade mechanism linking episodic experience to ripple reorganization and synaptic remodeling during memory encoding.

Keywords: hippocampus, episodic memory, ripple firing, synaptic plasticity, super burst, information entropy, memory encoding

INTRODUCTION

Every day we encounter events that encompass the elements of "when, where, and what." The hippocampus serves as the primary site for processing episodic memory (1), where spatiotemporal information (2,3) or specific episodes are represented (4). Specifically, CA1 neurons in the dorsal hippocampus encode the location and context in which an animal identifies novel environments (5), and transient inactivation of these neurons impairs performance on memory tests (6). Learning to avoid a stressful location necessitates synaptic plasticity in dorsal CA1 neurons (7,8). Additionally, CA1 neurons are essential for object recognition (9), and several junction place cells have been shown to represent information about the location of another animal when housed together (10). However, the mechanisms by which memory processes differentiate between distinct episodes and retain prior experience remain completely unknown.

CA1 neurons often synchronize with neighboring neurons during their functions, and the number of synchronizing neurons increases with task difficulty (11). Since the spatiotemporal firing patterns of multiple neurons can convey a neural code (12,13), large-scale electrophysiological activity of single neurons has been extensively studied (14). However, to analyze the firing activity behind ripples–thought to contain memory-related information–it is crucial to capture the coordinated firing activity of neighboring neurons with high spatiotemporal resolution. Isolating the synchronized firing activity of neighboring neurons that from a single ripple remains challenging. Moreover, the amplitude and shape of spikes can vary over time within the same neuron, particularly in burst-firing neurons (15). Additionally, dendritic plateau potentials and the complex burst firing they generate have been observed in learning animals (16). Therefore, in this study, we did not perform spike sorting; instead, we recorded the multi-unit firing activity of neighboring CA1 neurons in freely moving rats before and after the acquisition of episodic memory, examining the shape changes induced by the experienced episodes. By exposing animals to four episodes with different emotional content, our multiple-unit recording approach enabled episode-specific discrimination and captured temporal changes before and after the experiences.

Emotions such as happiness, fear, and sadness significantly influence memory strength (17-20), with these mechanisms relying on neurotransmission in the hippocampus. For instance, emotional arousal enhances learning thorough noradrenergic activation of dorsal CA1 neurons, which drives GluA1-containing AMPA receptors into synapses (21).

Additionally, tyrosine hydroxylase-expressing neurons in the locus coeruleus may facilitate memory by co-releasing dopamine in the hippocampus (22). However, conclusive evidence regarding whether emotional arousal influences the firing of CA1 neurons and their temporal dynamics in freely moving animals is still lacking. Furthermore, while many studies have established a causal relationship between synaptic plasticity and learning (7,8,23), conclusive evidence for spontaneous high-frequency firing during learning has yet to be observed.

In conjunction with excitatory synaptic plasticity, the maturation of inhibitory neurons has been shown to be essential for hippocampal learning (24,25). We recently discovered cell/tract-specific plasticity that positively correlates with acquired performance (26,27). Additionally, synaptic plasticity during the initial phase rapidly generates a diversity of excitatory and inhibitory postsynaptic currents within 10 minutes of experience, which are known to persist for over 60 minutes (28). Given that synaptic plasticity is a necessary process for generating rapid post-episodic diversity, we hypothesized that episode-specific diversity may arise to accommodate different types of episodes (29). To test this hypothesis, we examined the integrated plasticity of excitatory and inhibitory synapses in CA1 pyramidal neurons and found evidence for episode-type-specific diversity.

In this study, we identified three cellular and synaptic events that represent recent experiences in hippocampal CA1 neurons by monitoring multiple neural activities during learning and performing slice-patch clamp analyses.

RESULTS

Rats can learn experimental episodic memory

To mimic the events in humans that lead to episodic memory, adult male rats were exposed for 10 min to one of four different episodes (Fig. 1A): restraint stress, social interaction with a female or a male, and observation of a novel object (Fig. 1B). To assess acquired memory, the rats were re-exposed to the same episode and their behavior was assessed (30,31). Rats that experienced restraint stress showed fewer vocalizations during the second exposure (t_6 = 3.476, P = 0.0129). Similarly, rats exposed to a female, male, or novel object consistently reduced latency to vaginal inspection (t_8 = 3.492, P = 0.0082) or attack (t_7 = 4.192, P = 0.0041) and object observation time (t_9 = 2.901, P = 0.0176) during the second encounter, suggesting memory acquisition (32).

Multiple-unit activities and classification of firing patterns

To monitor the encoding process of the experience, we recorded multiple-unit firing activity from CA1 before (15 min), during (10 min), and after (30 min) each episode using an electrode that could record neural activity from many neighboring neurons (Figs. 1C and 1D). The number of recordings was no-experience control (N = 7), restraint stress (N = 9), contact with a female (N = 11), contact with a male (N = 11), and a novel object (N = 9). Although the neural activity could not separate multiple neurons into single units (Fig. S1), spike half-width analysis classified the 284 estimated well-separated single neurons, yielding 220 estimated pyramidal neurons (> 0.7 msec), 38 estimated interneurons (< 0.4 msec), and 26 unclassified neurons (0.4 to 0.7 msec), suggesting the location of the recording in the pyramidal cell layer (Fig. S1D). We found that neighboring CA1 neurons exhibited several unique firing patterns particularly after the onset of an episode. Based on the following criteria, we extracted the events of super bursts and ripple firings (Fig. 1E).

Prior to the experience, CA1 neurons showed mostly sporadic firings (Fig. 1F, Movie S1), with some ripple firings when the rats were in their home cage. Using the 100 - 300 seconds of low-noise data prior to the experience, we calculated the basal firing rate for each individual (n = 12390). We then extracted spontaneous high-frequency firings (Figs. 1E, 1G, 2A, and 2B), defining a super burst as one with a firing rate higher than three standard deviations (SDs) of the mean firing rate before the episode (n = 327). CA1 neurons often exhibited ripple firings separated by no-firing silent periods (Fig. 1H, Movie S2). We detected sharp-wave ripples (150 – 300 Hz), and in this study we analyzed the firing patterns behind them as ripple firings (300 – 10 kHz), showing short-duration (56.3 ± 16.5 msec ± SD, n = 5333), high-frequency clustered firings with a signal-to-noise ratio of at least 6:1 (Fig. 1I). Super bursts and ripple firings were clearly distinguished by their duration (Fig. 1E and S2).

Super bursts represent episode-type specific features

We started recording in the home cage before the experience, and examined changes in the occurrence and duration of super bursts with each episodic experience (Figs. 2C and 2D). To statistically evaluate this change, we used a two-way analysis of variance (ANOVA) with experience as the between-group factor and time as the within-group factor. The results showed a significant effect of episode (events 3 min^{-1}, $F_{4, 546}$ = 2.482, P = 0.058; duration, $F_{4, 546}$ = 3.145, P = 0.024), time (events 3 min^{-1}, $F_{13, 546}$ = 4.937,

$P < 0.0001$; duration, $F_{13, 546} = 7.288$, $P < 0.0001$), and their interaction (events 3 min^{-1}, $F_{52, 546} = 1.567$, $P = 0.009$; duration, $F_{52, 546} = 3.095$, $P < 0.0001$). To further analyze the effect of time in individual episodes, we performed *post hoc* ANOVAs. Both, the occurrence and duration were significantly increased by restraint (events 3 min^{-1}, $F_{13, 104} = 5.174$, $P < 0.0001$; duration, $F_{13, 104} = 7.697$, $P < 0.0001$), contact with a female (events 3 min^{-1}, $F_{13, 130} = 2.589$, $P = 0.0032$; duration, $F_{13, 130} = 2.852$, $P = 0.0012$), and contact with a male (events 3 min^{-1}, $F_{13, 130} = 1.940$, $P = 0.031$; duration, $F_{13, 130} = 1.880$, $P = 0.038$). In contrast, they remained unchanged after contact with a novel object (events 3 min^{-1}, $F_{13, 104} = 0.788$, $P = 0.671$; duration, $F_{13, 104} = 0.783$, $P = 0.676$), suggesting an episode-dependent generation of super bursts in neighboring CA1 neurons. No significant change was observed in the control group that did not experience episodes (events 3 min^{-1}, $F_{13, 78} = 0.844$, $P = 0.614$; duration, $F_{13, 78} = 1.093$, $P = 0.377$).

Finally, occurrence and duration of super burst at each time point were compared two-dimensionally using a two-way multivariate analysis of variance (MANOVA; Fig. 2C *vs* 2D) with experience as the between-group factor and time as the within-group factor. Two-way MANOVA ($F_{8, 1304} = 9.761$, $P < 0.0001$) and *post-hoc* MANOVAs further revealed episode-specific differences in 8 “experience *vs.* experience” pairs in each of the total 10 comparison pairs (Table 1, see also Figs. 2C,D).

To further investigate whether the features of individual super bursts differ between episodes, the duration and relative firing rate of individual super bursts were plotted (triangles in Fig. 2E) and the integrated two parameters analyzed by one-way MANOVA. The X-axis is the duration (sec) and the Y-axis is the firing frequency with pre-experience set to 1. MANOVA ($F_{8, 558} = 11.535$, $P < 0.0001$) and *post-hoc* MANOVAs revealed episode-specific differences in 6 “experience *vs.* experience” pairs in each of the total 10 comparison pairs (Table 1, see also Fig. 2E).

Episodic experience consistently increases no-firing silent periods

Since the silent period without firing highlighted the ripple firings (Fig. 3A), the silent period may be important to support memory processing. For the rate of silent period (Fig. 3B), a two-way ANOVA showed significance within time ($F_{2, 84} = 18.167$, $P < 0.0001$), but neither the main effect of experience ($F_{4, 84} = 1.006$, $P = 0.415$) nor the interaction was significant ($F_{8, 84} = 1.508$, $P = 0.167$). In the within-group temporal analysis, the rate of silent periods increased with restraint stress ($F_{2, 16} = 3.740$, $P = 0.047$) and contact with

female ($F_{2, 20}$ = 7.018, P = 0.005), male ($F_{2, 20}$ = 8.557, P = 0.002), and novel object ($F_{2, 16}$ = 6.063, P = 0.011). Episode consistently increased silent periods regardless of experience type, whereas no significant change was observed in the no-experience control ($F_{2, 12}$ = 0.534, P = 0.599) (Table S1; detailed ANOVA results for silent periods across episodes).

Changes in ripple firings depends on the nature of the episodic experience

Hippocampal ripple oscillations (140 – 250 Hz) are known as oscillatory patterns observed on an electroencephalogram during sleep or immobility that are important for memory and action planning. High frequency clustered firing appears in conjunction with ripple oscillations (33). Here, we recorded 300 – 10 kHz band to detect individual firings behind the ripples. Since the clustered firings by multiple neurons were almost all synchronized with a ripple, we defined the clustered firings as a “ripple firings”. To examine the episode-induced ripple firings, we first counted the occurrence.

For the occurrence of ripple firings (Fig. 3C), a two-way ANOVA showed significance within time ($F_{2, 84}$ = 10.649, P < 0.0001) and interaction ($F_{8, 84}$ = 3.422, P = 0.002), but the main effect of experience was not significant ($F_{4, 84}$ = 0.882, P = 0.483). We found a within-group temporal increase in the occurrence of ripple firings with restraint stress ($F_{2, 16}$ = 18.672, P < 0.0001) and contact with female ($F_{2, 20}$ = 6.908, P = 0.005) or male ($F_{2, 20}$ = 4.992, P = 0.017), while the occurrence decreased with novel object ($F_{2, 16}$ = 3.881, P = 0.042). Episodic experience altered the occurrence of ripple firings, depending on the nature of experience. In contrast, no significant change was observed in the no-experience control ($F_{2, 12}$ = 1.991, P = 0.179). Detailed ANOVA results for the occurrence of ripple firings across episodes were shown in Table S2.

Super bursts correlated more with ripple firings than with silent periods.

Depolarization of CA1 neurons is known to be the initial trigger of synaptic plasticity (34,35). Although an intrinsic spontaneous trigger has not been found in free-moving/learning animals, we were able to record super bursts especially during the emotional episode. Since not only excitatory/inhibitory synaptic transmission is necessary for ripple generation (33, 34-38), we predicted super bursts as an event that induces synaptic plasticity. To address this issue, we analyzed whether super bursts correlated with ripple firings or silent period in individual animals.

Although the increase in silent periods was not correlated with the number or total duration of super bursts (Figs. S3A and B), the increase in ripple firings was positively correlated with the number or total duration of super bursts (Figs. S3C and D).

The diversity of ripple firings represents recent experience

The ripple appears in conjunction with a sharp wave, and this oscillation is known as sharp-wave/ripple complexes (SPW-Rs). Suppression of SPW-Rs impairs learning and memory (39,40), and learning prolongs the duration of SPW-R (41). The firing sequence during SPW-Rs replays the sequence of the location during spatial learning (42), and spikes during SPW-R duration are increased by learning (41). These observations suggest that ripples contain learning information, and the firings that co-occur with ripples serve as an element. Because ripple firings are composed of many spikes from multiple neurons, we hypothesized that ripple firings might provide episode-type specific features representing the recent experience.

Here, we extracted four features from individual ripple firings (Fig. 3D) and analyzed them using two-way repeated measures of ANOVA, where a between-group factor was experience and a within-group factor was time (Fig. 3E). *Post-hoc* ANOVAs further showed the differences in temporal dynamics (Table S3; detailed ANOVA results in individual features across episodes). Values for all features mostly increased with episodic experience, but the number of peaks decreased after contact with a novel object. These changes were maintained for at least 40 min, while none of the four features changed in the no-experience control.

Based on Shannon's information theory, we also calculated the appearance probability of the four features (Fig. 3F). First, we determined the distribution of the appearance probability before the experience, followed by the analysis of the appearance probability of all ripple firings individually. The diversity of ripple firings expanded significantly with the experience, increasing the information entropy per single ripple-firings, and these changes were also maintained for at least 40 min (Fig. 3F). Two-way repeated measures of ANOVA showed overall significance on the 4 self-entropies of ripple firings, and *post-hoc* ANOVAs further showed the differences in temporal dynamics (Table S4; detailed ANOVA results for individual self-entropies across episodes.

Finally, we analyzed the episode-type specificity using MANOVA: the four features for each ripple-firings were integrated and the waveform diversification was evaluated

comprehensively. Due to the difficulty of plotting in four dimensions, individual ripple features were plotted in three dimensions (Fig. 3G), but the diversity of ripple firing was actually compared in four-dimensional distribution. Two-way MANOVA and *post-hoc* MANOVAs further revealed episode-specific differences in all "experience *vs.* experience" pairs in any of the total 10 comparison pairs. The temporal dynamics of ripple diversity strongly suggested that both episode-dependent and episode type-specific changes in the ripple firings in hippocampal CA1 neurons, while no significant temporal change was observed in the no-experience control (Table 2, see also Fig. 3G).

Similarly, the integrated four self-entropy data for each ripple firings were analyzed using MANOVA and *post-hoc* MANOVAs, suggesting episode-specific differences in all "experience *vs.* experience" pairs in any of the total 10 comparison pairs. These results indicate both episode-dependent and episode-type specific changes in the information entropy per single ripple-firings, while the overall temporal change in the no-experience control was not significant (Table 2, multi-dimensional self-entropy plot was not shown).

Furthermore, the post-experience features of ripple firings were significantly correlated with the number and total duration of super bursts in the same animal, but not with the pre-experience features of ripple firings. The results show that not only the number of ripple firings (Figs. S3C and D), but also the changes in their features were under the influence of the preceding events, the super bursts (Fig. 3H). Super bursts may contribute to the generation of new ripple firings after the episodic experience.

Episode-type specific diversification of postsynaptic currents at CA1 synapses

To further investigate experience-induced synaptic plasticity, we prepared brain slices for patch clamp analysis 40 min after the episodic experiences. By sequentially recording of mEPSCs (at −60 mV) and mIPSCs (at 0 mV) from the same neurons (29), we measured four parameters from individual CA1 neurons (Fig. 4A) and plotted them in virtual space (Fig. 4B): amplitudes and frequencies for both mEPSCs and mIPSCs. Postsynaptic currents are thought to correspond to the response elicited by a single vesicle of glutamate or GABA, while the number of synapses affects the frequency of events (43).

The results of one-way ANOVA on four individual parameters are shown in Figure 4C (Table S7; detailed ANOVA results across episodes). Although no experience controls showed a low and narrow distribution range of the synaptic strength, experience diversified it (Figs. 4B and D). Restraint stress increased both mEPSC and mIPSC amplitudes.

Contact with a female rat increased both amplitudes and mEPSC frequency. In contrast, contact with a male rat increased all four parameters, and contact with a novel object increased only mIPSC amplitude. These results suggest that the strength or number of excitatory and inhibitory synapses is altered depending on recent experience.

Finally, we analyzed the episode type specificity using MANOVA: the data from four features (amplitude/frequency of mEPSC/mIPSC) were integrated and comprehensively evaluated. Four-dimensional virtual plots revealed episode-type specific synaptic plasticity in individual CA1 neurons (Fig. 4B, $F_{16, 551} = 4.729$; $P < 0.001$). Table 3 shows the differences between two specific episodes: *post-hoc* MANOVAs revealed episode-specific differences in 9 “experience *vs.* experience” pairs in each of the total 10 comparison pairs (see also Fig. 4B).

Based on the Shannon entropy, we further quantified synaptic diversity by measuring the population differences in mE(I)PSC amplitude and frequency compared to no-experience controls (44). The diversity of synaptic input strength increased significantly with the experience, increasing the information entropy per individual CA1 neuron (Fig. 4E and Table S8; detailed ANOVA results across episodes).

Similarly, the integrated self-entropy data showed episode-type specific diversity at excitatory and inhibitory CA1 synapses (Fig. 4D, $F_{16, 551} = 4.361$; $P < 0.001$). Table 3 shows the differences in the self-entropy between two specific episodes: *post-hoc* MANOVAs revealed episode-specific differences in 9 “experience *vs.* experience” pairs in each of the total 10 comparison pairs (see also Fig. 4D).

DISCUSSION

Long-term potentiation, established over five decades ago as a synaptic model of learning and memory (34), has recently demonstrated causal validity through targeted optogenetic manipulation studies (8,23). However, a critical paradox persists between experimental induction paradigms and natural learning conditions: while exogenous high-frequency stimulation protocols (e.g. 100 Hz, 1 sec) with coordinated presynaptic activation and postsynaptic depolarization reliably induce synaptic strengthening (45,46), the endogenous sources of such precisely patterned activity in behaving animals remain unidentified. Our study addressed this fundamental question by characterizing spontaneous "super bursts" - self-organized high-frequency firing patterns (above 3 standard deviations of basal firing) in CA1 neurons that arise specifically during episodic encoding.

Acetylcholine (ACh) is one of the leading candidates for eliciting super bursts, known to induce plasticity at dorsal CA1 synapses (47,48). Indeed, both restraint stress and learning increase ACh release in the dorsal CA1 *in vivo* (29,49), and the positive correlation between ACh release and contextual fear performance is blocked by scopolamine (50). Furthermore, prior mechanistic studies have established that microinjections of ACh antagonists inhibit learning-induced synaptic plasticity, suggesting that ACh is essential for the induction of super bursts and subsequent synaptic diversity (29).

The features of post-experience ripple firings, but not pre-experience ripple firings, showed a significant correlation with the total number and duration of super bursts in the same animals (Fig. 3H). Additionally, experiencing an emotional episode significantly increased the occurrence of super bursts (Fig. 2), and excitatory synapses were strengthened in these groups (Fig. 4C). Based on these findings, we hypothesize a causal relationship between the diversification of post-super burst ripple firing in hippocampal CA1 neurons and subsequent memory acquisition (Fig. 5). To establish this causal relationship, it is essential to evaluate ripple firing diversity, synaptic plasticity, and learning ability while controlling for experience-induced super bursts. In a preliminary study, a causal relationship was suggested, as administration of scopolamine prior to restraint stress prevented the occurrence of super bursts, suppressed the diversity of ripple firings, and reduced freezing performance in the same subjects (51).

In contrast to restraint stress or social experiences, only inhibitory synaptic currents and silent periods increased in response to novel objects. More importantly, the increase in $GABA_A$ currents was not specific to novel objects. For all four types of episodic experiences, both inhibitory synaptic currents (Fig. 4C) and silent periods without firing (Fig. 3B) exhibited a consistent increase across the experience groups. Since novel elements are present in all four types of experiences, the consistent increase in inhibitory synaptic currents and the formation of silent periods may be essential for processing information related to novel objects and animals. While microinjection of higher doses of $GABA_A$ receptor agonists into CA1 impairs memory for novel objects (52,53), it is also known that suppression of neuronal activity can facilitate information processing (54, 55), and a decrease in background firing after an experience may emphasize ripple firings to convey information. Although the causal relationship between strengthening inhibitory synapses and increasing silent periods remains to be established, inhibitory synapses are recognized as necessary for learning and memory, as well as for ripple wave formation (24, 33, 56).

Sharp wave-ripple complexes (SPW-Rs) - high-frequency oscillations (140–250 Hz) coupled with sharp waves (33) - play fundamental roles in memory consolidation and behavioral planning (57,58). Experimental suppression of SPW-Rs consistently disrupts both learning acquisition and memory retrieval processes (39,40), whereas successful learning induces progressive prolongation of SPW-R durations (41). This bidirectional relationship strongly supports their mechanistic involvement in memory formation. Notably, SPW-Rs exhibit precise temporal replay of spatial navigation sequences (42) and show learning-dependent amplification of spike participation within the ripple cycle (41), further substantiating their role as hippocampal memory engrams. Given the frequent occurrence of plateau potentials in CA1 neurons during learning states (16), our study specifically investigates the 300–10 kHz frequency band to characterize unsorted multi-unit activity patterns underlying ripple-generation mechanisms.

Our investigation of high-frequency EEG dynamics surrounding episodic experiences revealed two distinct patterns of ripple activity modulation: experience-dependent global change and episode-specific reorganization across four quantitative features of ripple waveforms (amplitude, duration, arc length, and spike peaks; Figs. 3E-G). Comprehensive analysis of 82,601 ripple firings waveform pairs using Euclidean distance metrics revealed significant morphological specificity, with individual events retaining unique spatiotemporal signatures (Fig. S4). Crucially, our similarity network analysis identified single-parameter discriminability - inter-ripple distance thresholds successfully encoded recent experience categories (classification accuracy: 92.3 ± 4.1%, $P < 0.001$; Table S9; detailed ANOVA results across episodes). This parametric sensitivity to experience history provides mechanistic evidence for content-specific information encoding within hippocampal ripple diversity.

The roles of excitatory and inhibitory synaptic transmission in SPW-R generation (59-61) and spike regulation during ripples are well established (33). In hippocampal slice models, SPW-Rs originate from CA3, propagate to CA1, and are critically dependent on AMPA receptor activation - their pharmacological blockade abolishes SPW-R generation (37,38). Inhibitory mechanisms involve two key processes: (i) CA3 interneurons coordinate pyramidal cell phase-locking through $GABA_A$ receptor-mediated synchronous IPSCs (62), and (ii) pre-SWR inhibitory activity governs pyramidal cell spike timing and enables sequence pattern diversification (59). At the synaptic level, miniature events (mEPSCs/mIPSCs) reflect single vesicle glutamate/GABA release, with event frequency

modulated by synaptic number (43). Our study linked these findings to recent experience by demonstrating integrative plasticity at both synapse types, with two distinct patterns of synaptic modulation: experience-dependent change and episode-specific reorganization across four quantitative features of synaptic currents (mEPSC amplitude/frequency and mIPSC amplitude/frequency; Table 3).

Our model consists of three stages

Our experimental observations show that experience-dependent super bursts exhibit initial episode-type specificity in temporal organization patterns (Table 1). This leads us to propose a cascading plasticity model in which these patterned bursts: Establish experience-specific synaptic configurations through selective dendritic integration (Table 3), Shape ripple diversity by creating distinct excitation-inhibition balances across microcircuits (Table 2). While the causal relationships between experience, synaptic plasticity, and ripple dynamics require further elucidation, three lines of evidence support this framework: 1) Necessity of synaptic plasticity: Single-unit *in vivo* recordings show that NMDA receptor-dependent plasticity provides the cellular basis for encoding novel experience, as evidenced by impaired place field formation following plasticity blockade (63). 2) Memory-specific reorganization: Aversive stimuli induce rapid place cell remapping (≤ 5 minutes post-event), suggesting experience-driven reconfiguration of network firing motifs for memory storage (64). 3) Experience-structured replay: Large-scale neural ensemble analyses reveal that sequential replay events progress through distinct stages (exploration → consolidation → retrieval) with experience-dependent structured evolution (65).

In this study, we identified three distinct hippocampal CA1 events associated with the representation of recent experience. The functional hierarchy between CA3 and CA1 is most evident in ripple oscillations, the disruption of which is known to impair memory consolidation (39,40,66). Our results further suggest that sequential ripple firing patterns may coordinate the processing cascade for recent experiences (65). Although the causal mechanism requires further investigation, we recently reported the following: 1) Plasticity in inhibitory $GABA_A$ synapses is essential for contextual learning, 2) hippocampal commissure stimulation synchronized with super burst initiation blocks learning and synaptic diversification; and 3) optogenetic inhibition of cholinergic input to the hippocampus only during contextual experience specifically impairs learning in ChAT-Cre mice (67, 68). Based on these findings, we propose an experience-dependent information processing pathway

characterized by: i) ripple diversification following experience-specific super bursts, and ii) subsequent integrative plasticity at excitatory / inhibitory synapses. As illustrated in Figure 5, this model predicts that targeted modulation of these three events – particularly through temporal coordination of their activation patterns – could establish novel paradigms for memory enhancement. Future studies using precise optogenetic manipulation of these circuit elements could both validate this hypothesis and reveal potential therapeutic applications for memory disorders.

MATERIALS AND METHODS

Animals

Male Sprague-Dawley rats (CLEA Japan, Tokyo, Japan) were housed individually at 24 ± 1°C under a 12-hour light/dark cycle (lights on: 8:00 AM–8:00 PM) with ad libitum access to food (MF, Oriental Yeast Co. Ltd., Tokyo). Animals aged 15–25 weeks were used for *in vivo* recordings. Episodic stimuli were provided by 8–15-week-old male or female rats, housed separately without electrodes. All procedures were approved by the Yamaguchi University Animal Care and Use Committee and conformed to institutional and governmental regulations including the NIH Guide for the Care and Use of Laboratory Animals.

Surgery

Rats were anesthetized with sodium pentobarbital (50 mg/kg, i.p.) and placed in a stereotaxic frame. Movable tungsten electrodes (50–80 kΩ; KS-216, Unique Medical Co., Tokyo) were chronically implanted just above the dorsal CA1 region (AP: −3.0 to −3.6 mm; ML: ±1.4 to ±2.6 mm; DV: 2.0–2.2 mm) and secured with dental cement. Animals with incorrect electrode placements were excluded.

Multiple-unit Recording and Spike Detection

We started recording multiple-unit activity while the animals were in their familiar home cages and monitored their spontaneous behavior. Neural signals were recorded from the implanted electrodes via a headstage amplifier and shielded cable (MEG-2100 or MEG-6116; Nihon Kohden, Tokyo, Japan), filtered at 150–10,000 Hz, and digitized at 25 kHz using Spike2 software (Cambridge Electronics Design Ltd., Cambridge, UK).

Super bursts were defined as transient events with firing rates exceeding 3SD of baseline. Ripple firings were identified as short-duration (56.3 ± 16.5 msec ± SD, n = 5333)

high-frequency events (signal-to-noise ratio ≥ 6:1) following sharp-wave ripples (150–300 Hz). To detect sharp-wave ripples, we recorded signal (150–10 kHz) and filtered at 150–300 Hz and 300–10 kHz. Using the 150–300 Hz signal, we calculated the root mean square (RMS) and the threshold for the event detection was set to +6 SD above the mean of the baseline. Ripple firings were accompanied with the sharp-wave ripples. Grooming or teeth grinding show the characteristic of symmetrical amplitude of upper and lower peaks, and were excluded from the analysis.

Behavioral states during ripple firings were eye closed stationary 16.0 ± 7.0%, eye open stationary 59.7 ± 11.0%, or eye open moving 24.3 ± 11.3% (1631 events in 9 rats). Silent periods were defined as inter-spike intervals exceeding +3 SDs of baseline. For visual spike classification only (e.g., Fig. S1), template matching and spike width criteria were used to distinguish putative pyramidal neurons (>0.7 ms) from interneurons (<0.4 ms).

Behavioral Protocol and Recording Schedule

Following ≥15 min of baseline recording in the home cage, rats were exposed to one of four episodic conditions for 10 min: restraint stress, social interaction with a female or male, or exposure to a novel object (LEGO®/DUPLO® brick, 15×8×3 cm). Restraint involved tying the limbs with soft cloth and fixing the animal to a wooden board (49). Recordings continued for ≥30 min post-exposure. The next day, animals were re-exposed to the same episode for memory assessment (Fig. 1B).

Histology

After experiments, rats were deeply anesthetized (sodium pentobarbital 400 mg/kg, i.p.) and transcardially perfused with 0.1 M phosphate buffer containing 4% paraformaldehyde. Brains were post-fixed, cryoprotected in 10–30% sucrose, and sectioned coronally at 40 μm. Sections were stained with hematoxylin and eosin, and electrode placements were confirmed using a rat brain atlas (69).

Slice Patch-Clamp Recordings

Forty minutes after the start of episodic exposure, rats were deeply anesthetized, and coronal brain slices (350 μm) including CA1 were prepared using ice-cold dissection buffer and vibratome (Leica VT-1200). Slices were transferred to physiological recording solution (22–25°C, aerated with 5% CO_2/95% O_2). Whole-cell voltage-clamp recordings were

obtained from CA1 pyramidal neurons using pipettes (4–7 MΩ) filled with cesium-based internal solution.

Miniature excitatory (mEPSCs) and inhibitory (mIPSCs) synaptic currents were sequentially recorded at −60 mV and 0 mV, respectively, in the presence of 0.5 μM tetrodotoxin. AMPA and $GABA_A$ receptor blockers (CNQX, bicuculline, 10 μM each) confirmed event identity (29,44,70,71).

Quantification of Entropy and Statistical Analysis

The appearance probability of ripple waveform or synaptic features was estimated using one-dimensional kernel density analysis with Silverman's rule for bandwidth (72-74). Shannon entropy was computed in bits and log(1+x) transformed for parametric analysis (75). Statistical tests included one-way and two-way ANOVA, repeated-measures ANOVA, MANOVA (Wilks' lambda), and post hoc Fisher's LSD. Spearman's rank correlation was used to evaluate associations. Shapiro–Wilk and F tests assessed normality and variance homogeneity. Significance was set at $P < 0.05$.

ACKNOWLEDGMENTS The authors would like to thank Drs. Sora Takayama, Koushi Seo, and Ryo Sato for the comprehensive python analysis of ripple firings. This work was supported by Grant-in-Aid for Scientific Research B, 16H05129 (DM) and 19H03402 (DM), Grant-in-Aid for Scientific Research C, 26350988 (JI), 17K01987 (JI) and 25460314 (DM), and Scientific Research in Innovative Areas, 26115518 from the Ministry of Education, Culture, Sports, Science and Technology of Japan (DM). This project was also supported by YU AI project of center for information and data science education.

AUTHOR CONTRIBUTIONS DM and JI designed and performed the experiments. TT, JI, and DM analyzed firing events. DM and JI wrote the manuscript. DM organized the study, and all authors reviewed the manuscript.

SUPPLEMENTAL INFORMATION

Supplemental information can be found online. It is on the server of Yamaguchi University Graduate School of Medicine.

- Movie S1
- Movie S2

REFERENCES

1. Scoville WB, Milner B, Loss of recent memory after bilateral hippocampal lesions. J Neurol Neurosurg Psychiatry 20, 11–21 (1957).
2. O'Keefe J, Dostrovsky J. The hippocampus as a spatial map. Preliminary evidence from unit activity in the freely-moving rat. Brain Res. 34, 171-175, (1971).
3. Mitsushima D, Takase K, Funabashi T, Kimura F. Gonadal steroids maintain 24-h acetylcholine release in the hippocampus: organizational and activational effects in behaving rats. J. Neurosci, 29, 3808–3815 (2009).
4. Gelbard-Sagiv H, Mukamel R, Harel M, Malach R, Fried I, Internally generated reactivation of single neurons in human hippocampus during free recall. Science 322, 96–101 (2008).
5. Tanaka KZ, He H, Tomar A, Niisato K, Huang AJY, McHugh TJ, The hippocampal engram maps experience but not place. Science 361, 392–397 (2018).
6. Drieskens DC, Neves LR, Pugliane KC, De Souza IBMB, Lima ADC, Salvadori MGDSS, Ribeiro AM, Silva RH, Barbosa FF, CA1 inactivation impairs episodic-like memory in rats. Neurobiol. Learn. Mem. 145, 28–33 (2017).
7. Mitsushima D, Ishihara K, Sano A, Kessels HW, Takahashi T, Contextual learning requires synaptic AMPA receptor delivery in the hippocampus. Proc. Natl. Acad. Sci. U.S.A. 108, 12503–12508 (2011).
8. Goto A, Bota A, Miya K, Wang J, Tsukamoto S, Jiang X, Hirai D, Murayama M, Matsuda T, McHugh TJ, Nagai T, Hayashi Y, Stepwise synaptic plasticity events drive the early phase of memory consolidation. Science 374, 857-863 (2021).
9. Sun Y, Jin S, Lin X, Chen L, Qiao X, Jiang L, Zhou P, Johnston KG, Golshani P, Nie Q, Holmes TC, Nitz DA, Xu X, CA1-projecting subiculum neurons facilitate object-place learning. Nat Neurosci. 22, 1857-1870, (2019).
10. Danjo T, Toyoizumi T, Fujisawa S, Spatial representations of self and other in the hippocampus. Science. 359, 213-218, (2018).
11. Sakurai Y, Takahashi S, Conditioned enhancement of firing rates and synchrony of hippocampal neurons and firing rates of motor cortical neurons in rats. Eur. J. Neurosci. 37, 623–639 (2013).
12. Grinvald A, Arieli A, Tsodyks M, Kenet T, Neuronal assemblies: single cortical neurons are obedient members of a huge orchestra. Biopolymers 68, 422–436 (2003).
13. Kobayashi K, Matsuo N, Persistent representation of the environment in the

hippocampus. Cell Rep. 42**,** 111989 (2023).

14. Miyawaki H, Mizuseki K, De novo inter-regional coactivations of preconfigured local ensembles support memory. Nat. Commun. 13, 1272 (2022).
15. Einevoll GT, Franke F, Hagen E, Pouzat C, Harris KD, Towards reliable spike-train recordings from thousands of neurons with multielectrodes. Cur Opin Neurobiol 22, 11-17 (2012).
16. Bittner KC, Milstein AD, Grienberger C, Romani S, Magee JC, Behavioral time scale synaptic plasticity underlies CA1 place fields. Science 357, 1033-1036 (2017).
17. Christianson SA, The handbook of emotion and memory: research and theory. by Lawrence Erlbaum Associates, Inc. New Jersey (1992).
18. McGaugh JL, Memory – a century of consolidation. *Science* 287, 248–251 (2000).
19. Richter-Levin G, Akirav I, Emotional tagging of memory formation-in the search for neural mechanisms. Brain Res. Rev. 43, 247–256 (2003).
20. LeDoux JE, Emotion circuits in the brain. *Annu. Rev. Neurosci* **23**, 155–184. (2000).
21. Hu H, Real E, Takamiya K, Kang MG, Ledoux J, Huganir RL, Malinow R, Emotion enhances learning via norepinephrine regulation of AMPA-receptor trafficking. Cell 131, 160–173 (2007).
22. Takeuchi T, Duszkiewicz AJ, Sonneborn A, Spooner PA, Yamasaki M, Watanabe M, Smith CC, Fernández G, Deisseroth K, Greene RW, Morris RG, Locus coeruleus and dopaminergic consolidation of everyday memory. Nature 537, 357–362 (2016).
23. Ripoli C, Dagliyan O, Renna P, Pastore F, Paciello F, Sollazzo R, Rinaudo M, Battistoni M, Martini S, Tramutola A, Sattin A, Barone E, Saneyoshi T, Fellin T, Hayashi Y, Grassi C, Engineering memory with an extrinsically disordered kinase. Sci. Adv. 9, eadh1110 (2023).
24. Lovett-Barron M, Kaifosh P, Kheirbek MA, Danielson N, Zaremba JD, Reardon TR, Turi GF, Hen R, Zemelman BV, Losonczy A, Dendritic inhibition in the hippocampus supports fear learning. Science 343, 857–863 (2014).
25. Ramsaran AI, Wang Y, Golbabaei A, Aleshin S, de Snoo ML, Yeung BA, Rashid AJ, Awasthi A, Lau J, Tran LM, Ko SY, Abegg A, Duan LC, McKenzie C, Gallucci J, Ahmed M, Kaushik R, Dityatev A, Josselyn SA, Frankland PW, A shift in the mechanisms controlling hippocampal engram formation during brain maturation. Science 380, 543-551 (2023).
26. Yang Y, Sakimoto Y, Mitsushima D, Postnatal development of synaptic plasticity at

hippocampal CA1 synapses: correlation of learning performance with pathway-specific plasticity. Brain Sciences 14(4): 382. https://doi.org/10.3390/brainsci14040382 (2024).

27. Kida H, Toyoshima S, Kawakami R, Sakimoto Y, Mitsushima D. Properties of layer V pyramidal neurons in the primary motor cortex that represents acquired motor skills. Neuroscience, 559:54-63, 2024.
28. Sakimoto Y, Kida H, Mitsushima D, Temporal dynamics of learning-promoted synaptic diversity in CA1 pyramidal neurons. FASEB J. 33, 14382–14393 (2019).
29. Mitsushima D, Sano A, Takahashi T, A cholinergic trigger drives learning-induced plasticity at hippocampal synapses. Nat. Commun. 4, 2760 (2013).
30. Whishaw IQ, Kolb B, The behavior of the laboratory rat: a handbook with tests. Oxford University Press, NY (2005).
31. Mitsushima D, Yamada K, Takase K, Funabashi T, Kimura F, Sex differences in the basolateral amygdala: the extracellular levels of serotonin and dopamine, and their responses to restraint stress in rats. Eur. J. Neurosci. 24, 3245–3254 (2006).
32. Ishikawa J, Tomokage T, Mitsushima D, A possible coding for experience: ripple-like events and synaptic diversity. BioRxiv, 891259. (2019).
33. Buzsáki G, Hippocampal sharp wave-ripple: A cognitive biomarker for episodic memory and planning. Hippocampus 25, 1073–1188 (2015).
34. Bliss TV, Lømo T, Long-lasting potentiation of synaptic transmission in the dentate area of the anaesthetized rabbit following stimulation of the perforant path. J. Physiol. 232, 331–356 (1973).
35. Malenka RC, Nicoll RA, Long-term potentiation--a decade of progress? Science 285, 1870–1874 (1999).
36. Buzsáki G, Long-term changes of hippocampal sharp-waves following high frequency afferent activation. Brain Res 300, 179–182 (1984).
37. Behrens CJ, van den Boom LP, de Hoz L, Friedman A, Heinemann U, Induction of sharp wave-ripple complexes in vitro and reorganization of hippocampal networks. Nat. Neurosci. 8,1560–1567 (2005).
38. Schlingloff D, Kali S, Freund TF, Hajos N, Gulyás AI, Mechanisms of sharp wave initiation and ripple generation. J. Neurosci. 34, 11385–11398 (2014).
39. Girardeau G, Benchenane K, Wiener SI, Buzsáki G, Zugaro MB, Selective suppression of hippocampal ripples impairs spatial memory. Nat. Neurosci. 12, 1222–1223 (2009).

40. Jadhav SP, Kemere C, German PW, Frank LM, Awake hippocampal sharp-wave ripples support spatial memory. Science 336, 1454–1458 (2012).
41. Fernández-Ruiz A, Oliva A, Fermino de Oliveira E, Rocha-Almeida F, Tingley D, Buzsáki G, Long-duration hippocampal sharp-wave ripples improve memory. Science 364, 1082–1086 (2019).
42. Foster DJ, Wilson MA, Reverse replay of behavioural sequences in hippocampal place cells during the awake state. Nature 440, 680–683 (2006)
43. Pinheiro PS, Mulle C, Presynaptic glutamate receptors: physiological functions and mechanisms of action. Nat. Rev. Neurosci. 9, 423–436 (2008).
44. Sakimoto Y, Shintani A, Yoshiura D, Goshima M, Kida H, Mitsushima D, A critical period for learning and plastic changes at hippocampal CA1 synapses. Sci. Rep. 12, 7199, doi: 10.1038/s41598-022-10453-z, (2022).
45. Teyler TJ, Perkins AT 4th, Harris KM, The development of long-term potentiation in hippocampus and neocortex. Neuropsychologia 27, 31–39 (1989).
46. Malenka RC, Nicoll RA, Long-term potentiation--a decade of progress? Science 285, 1870–1874 (1999).
47. Auerbach JM, Segal M, Muscarinic receptors mediating depression and long-term potentiation in rat hippocampus. J. Physiol. 492, 479-493, (1996).
48. Fisahn A, Pike FG, Buhl EH, Paulsen O, Cholinergic induction of network oscillations at 40 Hz in the hippocampus in vitro. Nature 394, 186-189 (1998).
49. Mitsushima D, Takase K, Funabashi T, Kimura F, Gonadal steroid hormones maintain the stress-induced acetylcholine release in the hippocampus: simultaneous measurements of the extracellular acetylcholine and serum corticosterone levels in the same subjects. Endocrinology 149, 802-811 (2008).
50. Takase K, Sakimoto Y, Kimura F, Mitsushima D. Developmental trajectory of contextual learning and 24-h acetylcholine release in the hippocampus. Sci. Rep. 4, 3738 doi:10.1038/ srep03738, (2014).
51. Ishikawa J, Mitsushima D. Causality between spontaneous high-frequency firing "super bursts" of CA1 neurons and contextual learning. Neuro2024. 2P-201 (2024).
52. Yousefi B, Farjad M, Nasehi M, Zarrindast MR, Involvement of the CA1 $GABA_A$ receptors in ACPA-induced impairment of spatial and non-spatial novelty detection in mice. Neurobiol. Learn. Mem. 100, 32–40 (2013).
53. Cohen SJ, Munchow AH, Rios LM, Zhang G, Asgeirsdóttir HN, Stackman RW Jr., The

rodent hippocampus is essential for nonspatial object memory. Curr Biol. 23, 1685–1690 (2013).

54. Fairhall AL, Lewen GD, Bialek W, de Ruyter Van Steveninck RR, Efficiency and ambiguity in an adaptive neural code. Nature. 412, 787-92, (2001).
55. Reynolds JH, Heeger DJ, The normalization model of attention. Neuron. 61, 168-185, (2009)
56. Jeong N, Singer AC, Learning from inhibition: Functional roles of hippocampal CA1 inhibition in spatial learning and memory. *Curr Opin Neurobiol*. 343, 857-863, (2022).
57. Staresina BP, Wimber M, A neural chronometry of memory recall. Trends Cogn. Sci. 23, 1071-1085 (2019).
58. Zhang Y, Cao L, Varga V, Jing M, Karadas M, Li Y, Buzsáki G, Cholinergic suppression of hippocampal sharp-wave ripples impairs working memory. Proc. Natl. Acad. Sci. U.S.A. 118, e2016432118 (2021).
59. Noguchi A, Huszár R, Morikawa S, Buzsáki G, Ikegaya Y, Inhibition allocates spikes during hippocampal ripples. Nat. Commun. 13, 1280. doi: 10.1038/s41467-022-28890-28899 (2022).
60. Szabo GG, Farrell JS, Dudok B, Hou WH, Ortiz AL, Varga C, Moolchand P, Gulsever CI, Gschwind T, Dimidschstein J, Capogna M, Soltesz I, Ripple-selective GABAergic projection cells in the hippocampus. Neuron 110, 1959-1977 (2022).
61. Vancura B, Geiller T, Grosmark A, Zhao V, Losonczy A, Inhibitory control of sharp-wave ripple duration during learning in hippocampal recurrent networks. Nat. Neurosci. 26, 788–797 (2023)
62. Ellender TJ, Nissen W, Colgin LL, Mann EO, Paulsen O, Priming of hippocampal population bursts by individual perisomatic-targeting interneurons. J. Neurosci. 30, 5979–5991 (2010).
63. Bittner KC, Milstein AD, Grienberger C, Romani S, Magee JC, Behavioral time scale synaptic plasticity underlies CA1 place fields. Science 357:1033–1036 (2017).
64. Blair GJ, Guo C, Wang S, Fanselow MS, Golshani P, Aharoni D, Blair HT, Hippocampal place cell remapping occurs with memory storage of aversive experiences. eLife, e80661 (2023).
65. Mallory CS, Widloski J, Foster DJ. The time course and organization of hippocampal replay. Science 387: 541-548 (2025).
66. Norimoto H, Makino K, Gao M, Shikano Y, Okamoto K, Ishikawa Y, Sasaki T, Hioki H,

Fujisawa S, Ikegaya Y, Hippocampal ripples down-regulate synapses. Science 359, 1524-1527 (2018).

67. Sakimoto Y, Yang Y, Kida H, Mitsushima D, Phosphorylation of $GABA_A$ receptor β_3 subunit at $Ser^{408-409}$ is essential for contextual learning at hippocampal CA1 synapses. Sci. Rep. 15, 21525 (2025).
68. Yang Y, Ishikawa J, Mitsushima D, Super bursts reorganize hippocampal firing and promote synaptic diversity during stress-induced memory encoding. Soc. Neurosci. Abstr. C45 (2025).
69. Paxinos G, Watson C, The Rat Brain in Stereotaxic Coordinates., 6th edn., Academic Press, San Diego (2006).
70. Kida H, Tsuda Y, Ito N, Yamamoto Y, Owada Y, Kamiya Y, Mitsushima, D, Motor training promotes both synaptic and intrinsic plasticity of layer II/III pyramidal neurons in the primary motor cortex. Cereb. Cortex 26, 3494-3507 (2016).
71. Kida H, Kawakami R, Sakai K, Otaku H, Imamura K, Han-Thiri-Zin, Sakimoto Y, Mitsushima D, Motor training promotes both synaptic and intrinsic plasticity of layer V pyramidal neurons in the primary motor cortex. J. Physiol. 601, 335-353 (2023).
72. Sakimoto Y, Mizuno J, Kida H, Kamiya Y, Ono Y, Mitsushima D, Learning promotes subfield-specific synaptic diversity in hippocampal CA1 neurons. Cereb. Cortex 29, 2183–2195 (2019).
73. Sheather SJ, Density estimation. Statist. Science 19, 588–597 (2004).
74. Silverman BW, Density estimation for statistics and data analysis. Monographs on statistics and applied probability. Chaoman and Hall, London (1986).
75. Mitsushima D, Hei D, Terasawa E, γ-Aminobutyric acid is an inhibitory neurotransmitter restricting the release of luteinizing-hormone releasing hormone before the onset of puberty. Proc. Natl. Acad. Sci. U.S.A. 91, 395-399 (1994).

Figures and the legends

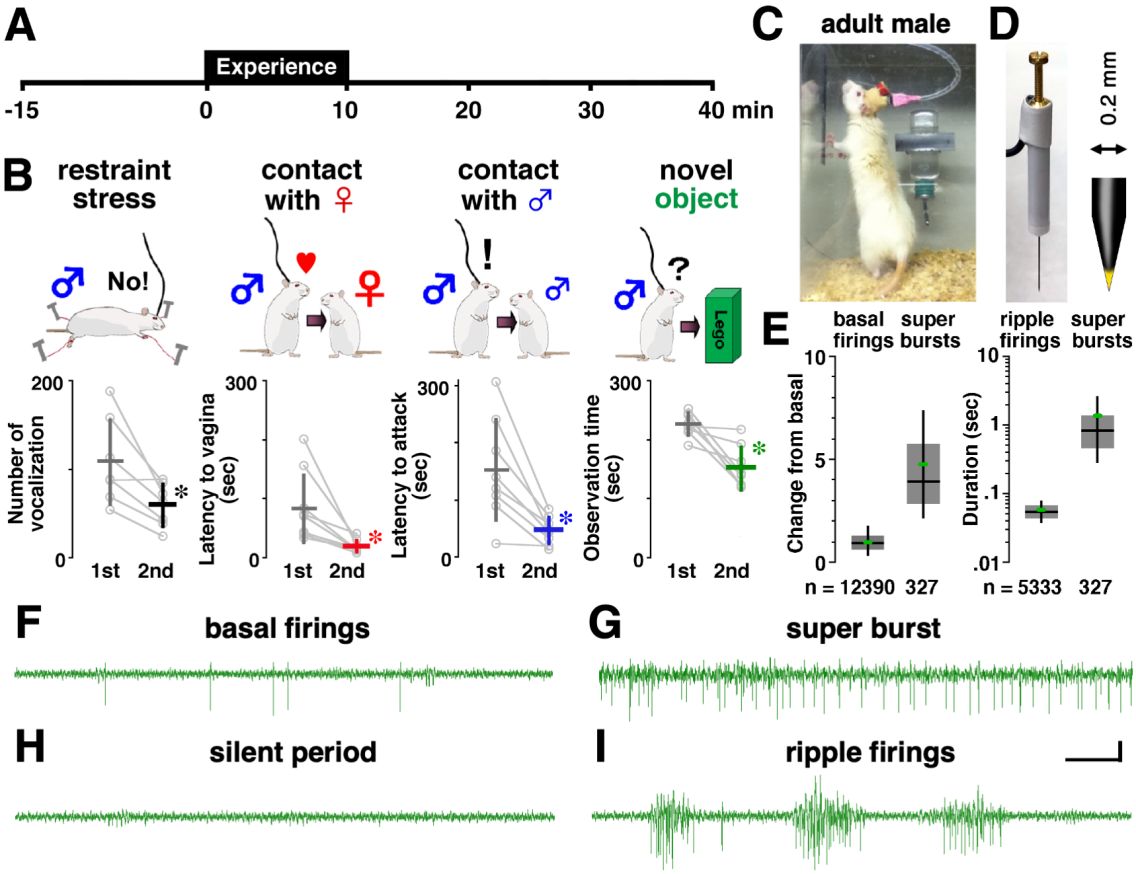

Figure 1. Experimental design for episodic memory and classification of CA1 multi-unit firing patterns. (A) Timeline of recording sessions and 10-minute episodic exposures. **(B)** Schematic illustrations of the four episodic experiences. Memory acquisition was assessed on the following day (2nd exposure). Data are shown as mean ± SD; gray circles represent individual rats with lines indicating within-subject changes. *P < 0.05 vs. 1st exposure. **(C)** Photograph of a recorded animal. **(D)** Movable recording electrode with an enlarged tip. **(E)** Features of super bursts and ripple firings. The box indicates 50% central area with a line that represents the median. The vertical line indicates minimum to maximum data area without outliers. The green dot represents the average. Sample size (number of events) is indicated below each bar. **(F–I)** Examples of multiple-unit activity from CA1 recorded at 25 kHz and filtered between 300–10,000 Hz. These traces were recorded from an electrode that was implanted in the same animal. **(F)** Basal firings. **(G)** Super burst. **(H)** Silent period. **(I)** Ripple firings (three examples). Note: Spike classification using the Spike2 algorithm is unreliable during super bursts and ripple firings (see Fig. S1). Scale bar = 50 ms.

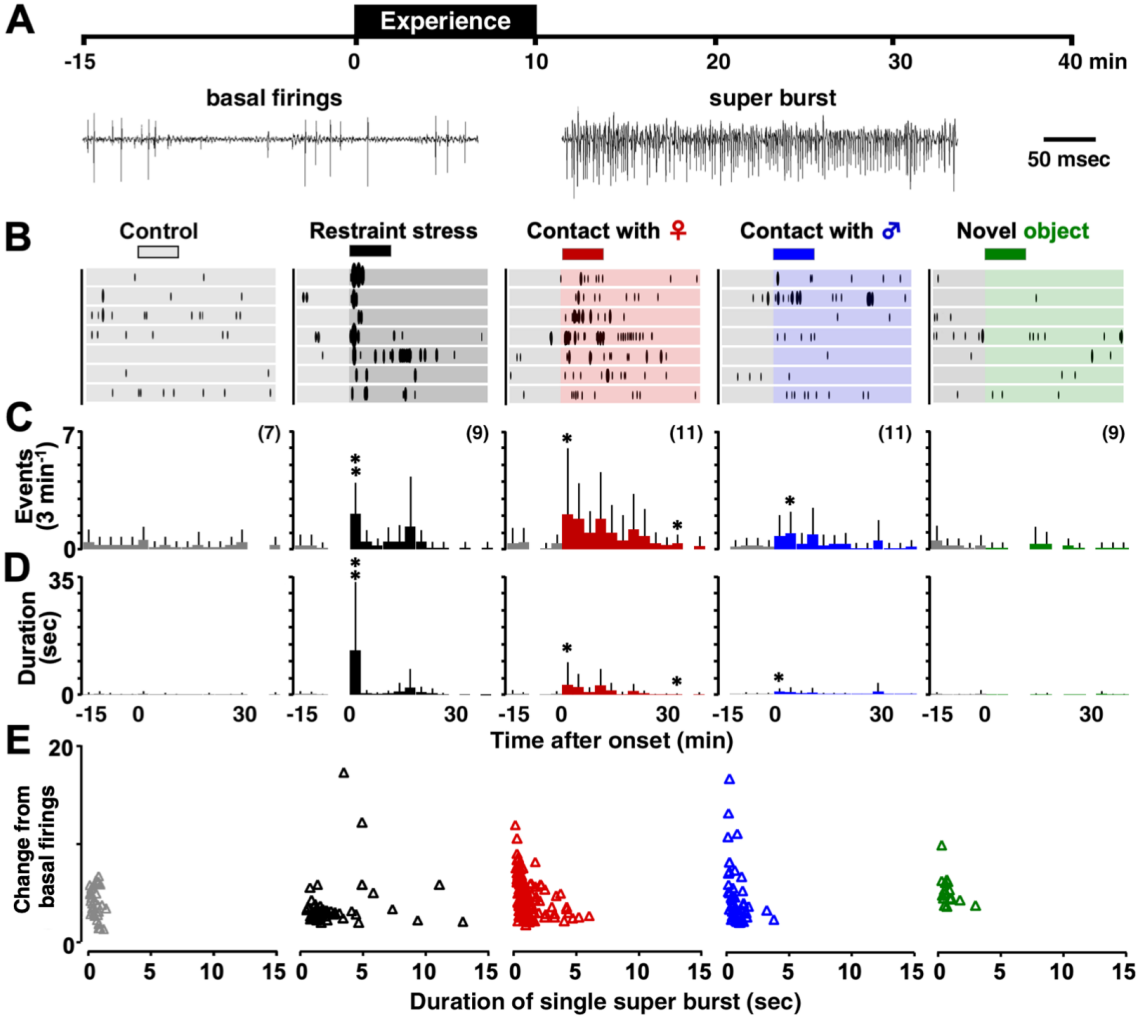

Figure 2. Experience-dependent induction of high-frequency CA1 multi-unit firing (super bursts). (A) Representative trace showing baseline firing and an episode-induced super burst in CA1 neurons. **(B)** Time course of super burst occurrences before, during, and after episodic experiences in individual animals. Horizontal black bars indicate the 10-min episode window. **(C–D)** Quantification of the occurrence (C) and total duration (D) of super bursts in 3-min bins across time. **(E)** Scatter plots of individual super burst events, showing episode-specific differences in duration (x-axis) and normalized firing rate (y-axis). Multidimensional analysis of the features showed distinct patterns based on episode type (Table 1, by MANOVA). Pre-experience baseline is set to 1. Data are shown as mean ± SD. The number of recordings in each group is shown in parentheses. *P < 0.05, **P < 0.01 vs. pre-experience baseline.

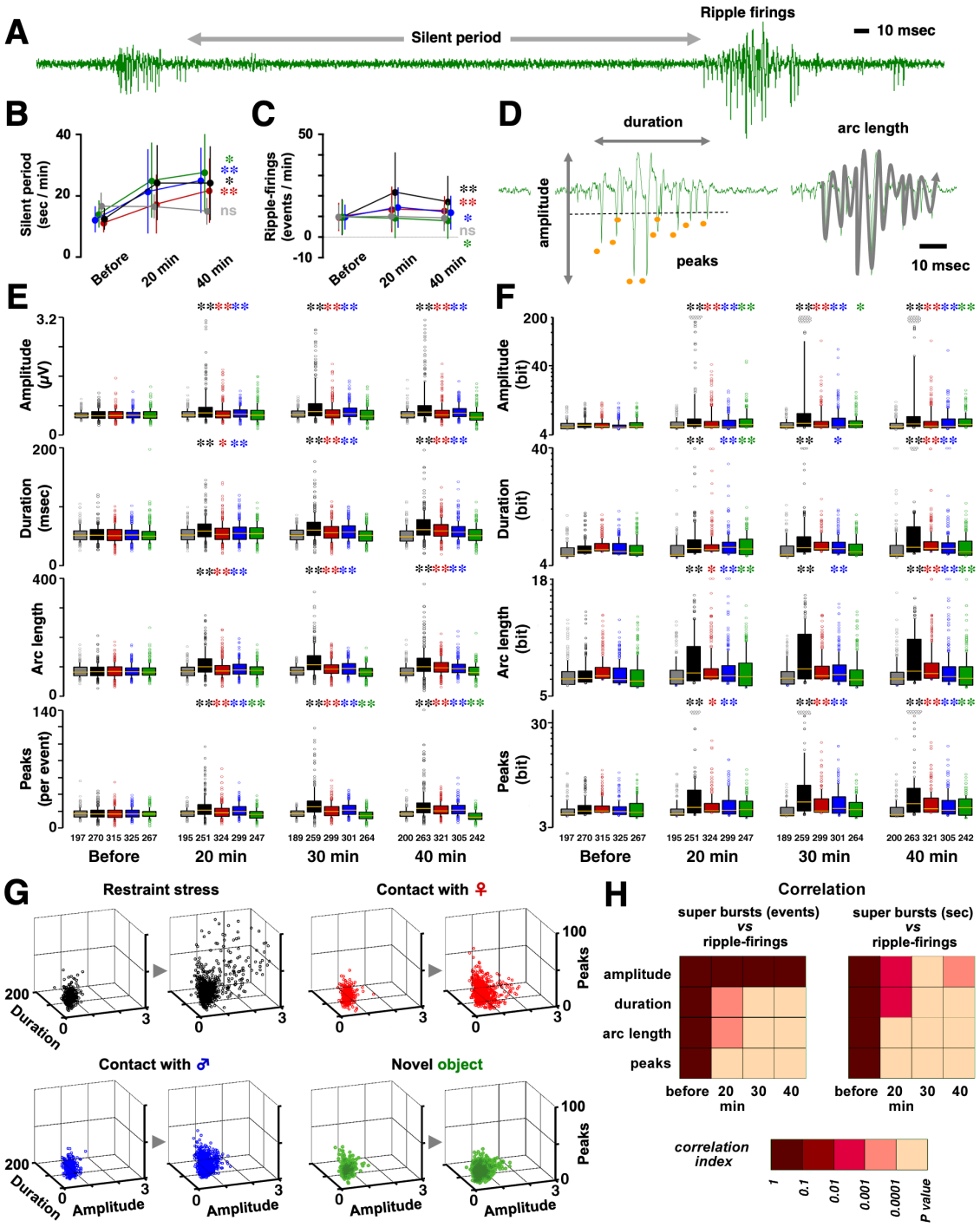

Figure 3. Experience-dependent diversification of ripple firings in CA1 neurons. (A) Example trace showing a silent period flanked by two ripple firings. **(B–C)** Episodic experience increased the total duration of silent periods (B) and the occurrence of ripple firings (C). Data are shown as mean ± SD. **(D)** Four extracted features of ripple firings: amplitude, duration, arc length, and number of negative peaks. **(E)** Temporal dynamics of each ripple firing feature across conditions, showing episode-dependent modulation. The box indicates 50% central area with a line that represents the median. The vertical line indicates

minimum to maximum data area without outliers. Sample size (number of ripple firing) is indicated below each bar. **(F)** Information entropy per ripple firing, derived from the distribution of waveform features, increased after experience. **(G)** Multidimensional analysis of the four features revealed distinct clustering patterns based on episode type (Table 2, by MANOVA, graphs show selected three dimensions). **(H)** Correlations between super bursts and ripple features before (left) and after (right) the experience. Only post-experience features showed significant correlation. *$P < 0.05$, **$P < 0.01$ vs. pre-experience.

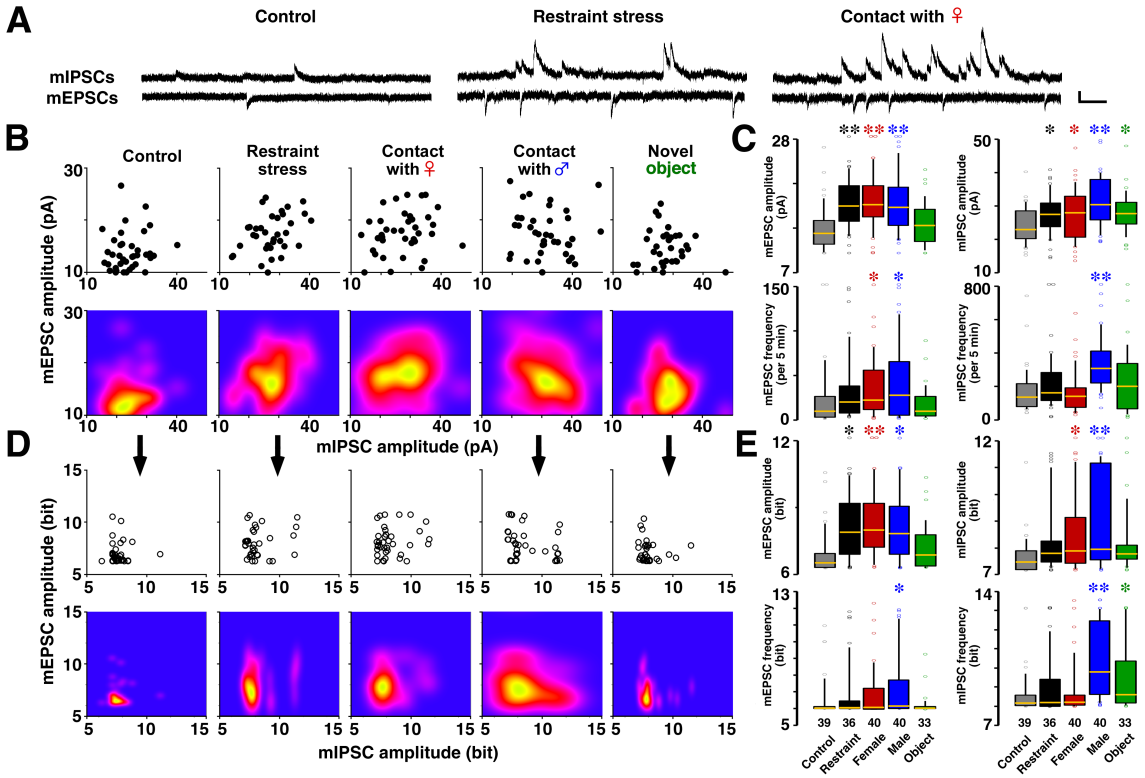

Figure 4. Experience-specific synaptic plasticity at excitatory and inhibitory CA1 synapses. (A) Representative traces of miniature excitatory (mEPSCs, top) and inhibitory (mIPSCs, bottom) postsynaptic currents from the same CA1 neuron. **(B)** Mean amplitudes of mEPSCs and mIPSCs (top), and their density distribution (bottom). Although only two dimensions are shown, four-dimensional analysis (including frequency data) revealed episode type-specific differences (Table 3, by MANOVA). **(C)** Box plots showing experience-dependent changes in the four synaptic parameters: amplitude and frequency of mEPSCs and mIPSCs (by ANOVA). **(D)** Information entropy for each neuron, calculated from the four synaptic features, showed episode type-specific diversification (Table 3, by MANOVA). **(E)** Box plots of individual self-entropy parameters (by ANOVA). The box indicates 50% central area with a line that represents the median. The vertical line indicates minimum to maximum data area without outliers. Sample size (number of neurons) is indicated below each bar. *P < 0.05, **P < 0.01 vs. control.

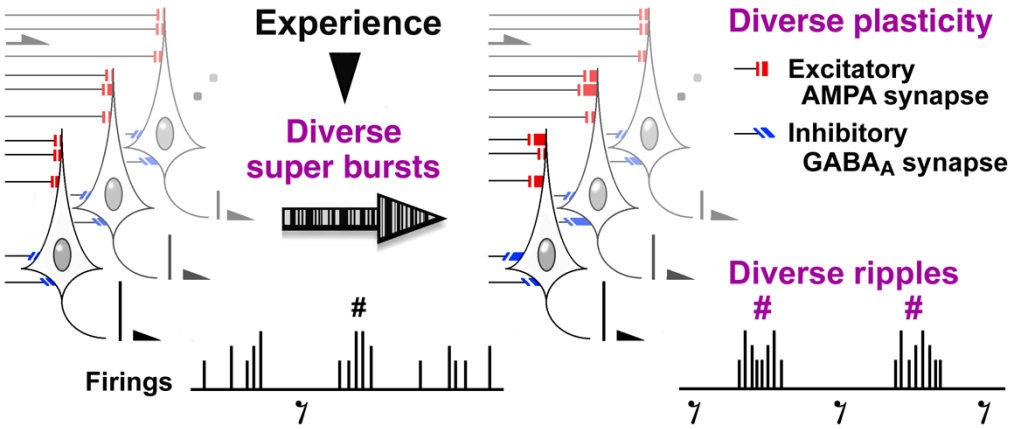

Figure 5. A proposed model for CA1 encoding of episodic experiences. After exposure to distinct episodes, CA1 neurons exhibit experience-specific patterns of high-frequency firing (super bursts), which may induce synaptic reorganization. This synaptic diversification in turn shapes the diversity of ripple firings (*sharp*), while increased inhibitory synaptic strength contributes to silent period formation (*rest*). This cascade may underlie the encoding of recent experience in hippocampal circuits. Illustration not drawn to scale. See Discussion for detailed explanation. Note that CA1 contains over 400,000 and 5,000,000 pyramidal cells in rats and humans, respectively.

Table 1. Distinct super burst patterns emerge during episodic experience: MANOVA and post hoc analysis (related to Fig. 2).

Comparison	Figs 2C & 2D	Figure 2E
Overall	$F_{8, 1304} = 9.761$, $P < 0.001$**	$F_{8, 558} = 11.535$, $P < 0.001$**
Restraint *vs* Female	$F_{2, 277} = 14.066$, $P < 0.001$**	$F_{2, 177} = 24.009$, $P < 0.001$**
Restraint *vs* Male	$F_{2, 277} = 12.948$, $P < 0.001$**	$F_{2, 107} = 20.873$, $P < 0.001$**
Restraint *vs* Object	$F_{2, 249} = 8.367$, $P < 0.001$**	$F_{2, 66} = 19.088$, $P < 0.001$**
Restraint *vs* Control	$F_{2, 221} = 9.517$, $P < 0.001$**	$F_{2, 82} = 33.336$, $P < 0.001$**
Female *vs* Male	$F_{2, 305} = 4.793$, $P < 0.001$**	$F_{2, 181} = 6.037$, $P = 0.003$**
Female *vs* Object	$F_{2, 277} = 13.075$, $P < 0.001$**	$F_{2, 140} = 1.589$, $P = 0.208$
Female *vs* Control	$F_{2, 249} = 7.004$, $P < 0.001$**	$F_{2, 156} = 4.695$, $P = 0.011$*
Male *vs* Object	$F_{2, 277} = 5.160$, $P = 0.006$**	$F_{2, 70} = 1.912$, $P = 0.155$
Male *vs* Control	$F_{2, 249} = 1.248$, $P = 0.289$	$F_{2, 86} = 2.806$, $P = 0.066$
Object *vs* Control	$F_{2, 221} = 1.916$, $P = 0.150$	$F_{2, 45} = 0.445$, $P = 0.644$

Summary of MANOVA and subsequent post hoc tests comparing the integrated features (incidence *vs* duration or frequency *vs* duration) of super bursts across different episodic experiences. Significant differences highlight experience-specific modulation of ensemble-level high-frequency firing.

Table 2. Episodic experience diversifies ripple firing features: MANOVA and post hoc analysis (related to Fig. 3)

Comparison	Integrated features	Integrated self-entropies
Overall	$F_{12,\ 11993} = 48.996$, $P < 0.001$**	$F_{16,\ 16223} = 35.748$, $P < 0.001$**
Restraint *vs* Female	$F_{4,\ 2291} = 30.810$, $P < 0.001$**	$F_{4,\ 2291} = 33.374$, $P < 0.001$**
Restraint *vs* Male	$F_{4,\ 2262} = 31.515$, $P < 0.001$**	$F_{4,\ 2262} = 42.701$, $P < 0.001$**
Restraint *vs* Object	$F_{4,\ 2052} = 86.412$, $P < 0.001$**	$F_{4,\ 2052} = 48.154$, $P < 0.001$**
Restraint *vs* Control	$F_{4,\ 1813} = 48.846$, $P < 0.001$**	$F_{4,\ 1813} = 52.735$, $P < 0.001$**
Female *vs* Male	$F_{4,\ 2478} = 3.395$, $P = 0.009$**	$F_{4,\ 2478} = 3.920$, $P = 0.004$**
Female *vs* Object	$F_{4,\ 2268} = 60.959$, $P < 0.001$**	$F_{4,\ 2268} = 12.403$, $P < 0.001$**
Female *vs* Control	$F_{4,\ 2029} = 18.258$, $P < 0.001$**	$F_{4,\ 2029} = 43.749$, $P < 0.001$**
Male *vs* Object	$F_{4,\ 2239} = 94.403$, $P < 0.001$**	$F_{4,\ 2239} = 6.812$, $P < 0.001$**
Male *vs* Control	$F_{4,\ 2000} = 32.546$, $P < 0.001$**	$F_{4,\ 2000} = 31.836$, $P < 0.001$**
Object *vs* Control	$F_{4,\ 1790} = 23.418$, $P < 0.001$**	$F_{4,\ 1790} = 29.895$, $P < 0.001$**

Summary of MANOVA and subsequent post hoc tests comparing integrated ripple features (amplitude, duration, arc length, and number of negative peaks) following different episodic experiences. Increased variability and entropy measures indicate enhanced neural representation diversity. Detailed statistical results were shown in Tables S5 (integrated features) and S6 (integrated self-entropies). Significant differences highlight experience-specific features of ripple firings and the diversity.

Table 3. Experience-specific reorganization of excitatory and inhibitory synaptic inputs: MANOVA and post hoc analysis (related to Fig. 4)

Comparison	Synaptic parameters	Self-entropies
Overall	$F_{16, 551} = 4.729$, $P < 0.001$**	$F_{16, 551} = 4.361$, $P < 0.001$
Restraint *vs* Female	$F_{4,71} = 0.834$, $P = 0.508$	$F_{4,71} = 0.623$, $P = 0.648$
Restraint *vs* Male	$F_{4,71} = 4.046$, $P = 0.005$**	$F_{4,71} = 4.188$, $P = 0.004$**
Restraint *vs* Object	$F_{4,64} = 3.353$, $P = 0.015$*	$F_{4,64} = 2.821$, $P = 0.032$*
Restraint *vs* Control	$F_{4,70} = 5.305$, $P < 0.001$**	$F_{4,70} = 3.834$, $P = 0.007$**
Female *vs* Male	$F_{4,75} = 9.592$, $P < 0.001$**	$F_{4,75} = 5.821$, $P < 0.001$**
Female *vs* Object	$F_{4,68} = 5.049$, $P < 0.001$**	$F_{4,68} = 4.092$, $P = 0.005$**
Female *vs* Control	$F_{4,74} = 5.729$, $P < 0.001$**	$F_{4,74} = 4.497$, $P = 0.003$**
Male *vs* Object	$F_{4,68} = 4.794$, $P = 0.002$**	$F_{4,68} = 5.141$, $P < 0.001$**
Male *vs* Control	$F_{4,74} = 15.762$, $P < 0.001$**	$F_{4,74} = 13.174$, $P < 0.001$**
Object *vs* Control	$F_{4,67} = 3.767$, $P = 0.008$**	$F_{4,67} = 2.988$, $P = 0.025$**

Summary of MANOVA and subsequent post hoc tests comparing integrated excitatory and inhibitory synaptic current parameters (amplitude and frequency of mEPSCs and mIPSCs) recorded *ex vivo* from CA1 pyramidal neurons. Significant differences highlight experience-specific features of integrated synaptic remodeling and the diversity.